Modification of surface layers of polymers by ion beams

Popok, Vladimir

Published in:
Surface Investigation

Publication date:
1999

Document Version
Publisher's PDF, also known as Version of record

Surface Investigation, 1999, Vol. 14, pp. 843–859
Reprints available directly from the publisher
Photocopying permitted by license only

Modification of Surface Layers of Polymers by Ion Beams

V. N. Popok

Belorussian State University, Minsk, Belarus

Received 8 August, 1996; accepted 24 February, 1997

The paper presents an analytical review of the literature data on the studies of near-surface polymer layers modified by ion implantation and diffusion doping with the aim to confer conducting properties on it. The accent is put on the nuclear physics research methods which are non-destructive and informative in the investigations of the polymer structure and composition. Peculiarities of the depth distribution of dopants, and possible mechanisms and models of their diffusion have been discussed. The main trends in the changes of the structure and composition of the modified polymer layer as a function of the implantation conditions, and the interrelation between the structural changes and profiles of the depth distribution of dopants have been considered.

IMPLANTED POLYMERS AS A NEW CLASS OF CONDUCTING MATERIALS

For different purposes in electronics it is necessary to have materials which combine properties of traditional inorganic semiconductors and the polymer medium. The first works bearing witness to the possibility of the production of conducting polymers have been published rather long ago [1, 2]. However, this research direction has received a new impulse only in the last two decades, when the electron conductivity of polymers was detected and technological possibilities arose for polymer production in the form of thin homogeneous films with prescribed reproducible parameters. [3].

The possibility to make electrically conducting layers in polymer films by their modification by ion beams and the following chemical doping has been actively studied in the recent years. The investigations in this direction have demonstrated the possibility of forming electrically conducting structures based on polymers which are dielectrics [4], and to control efficiently the conductivity by applying an external transverse electrical field [5]. However, because of the complex polymer structure and, also, the ambiguity of its change

at the implantation, there is no so far generally accepted view on the mechanisms of the charge carrier transport in the polymers modified by ion implantation [6, 7]. Moreover, which changes of the polymer matrix lead to the conductivity growth at the implantation is being actively discussed at the present time.

The use of implanted polymers is not restricted to microelectronics. Investigations of optical properties of implanted polymer materials to produce light filters [8, 9] and integral optical units [10, 11] are promising. The surface strengthening of polymers due to the implantation deserves attention [12, 13]. The ion bombardment can become one of the possibilities to control the bio-compatibility of polymer materials by the formation of surface pores and the destruction or creation of the centers of specific adsorption of alive cells [14, 15]. All these directions require independent investigations and analysis. We will not specially dwell on it in the presented work. It is necessary to note only that the above-enumerated possibilities of the application of implantation-modified polymers require a detailed study of structural changes, namely since they are liable for the change in the properties of these materials.

In connection with the above-said, a comprehensive study of the processes of the distribution of impurities introduced by implantation and diffusion and the accompanying changes in the structure and composition of polymer near-surface layers is of great interest.

Some of the nuclear analytical methods are used most often to investigate the structural peculiarities and distribution of dopants in polymer films. These methods include, for example, the Rutherford Back Scattering (RBS) technique [16, 17] and the analysis by nuclear reactions, in particular, the Neutron Depth Profiling (NDP) [18]. The advantage of RBS and NDP methods over others is that they are non-destructive or quasi-non-destructive. Last years the technique of these experiments as applied to the modified polymers has actively developed [4, 19–22].

In the present work the literature data concerning the problems of modification of the structure, composition and characteristics of polymer films subjected to the ion implantation and the following diffusion to obtain electrically conducting layers have been discussed and summarized.

DISTRIBUTION OF IMPURITIES INTRODUCED IN POLYMERS BY IMPLANTATION AND DIFFUSION

In most cases the experimentally obtained depth distribution profiles of ions introduced in polymers differ significantly from those calculated theoretically with the use of, for example, the TRIM program [23]. In the case of the implantation of light ions Li^+, B^+, F^+, the experimental depth distribution profiles correspond well to the calculated profiles of energy losses due to the ion deceleration by electrons [24]. Such a form of profiles is explained by redistribution of ions immediately after deceleration. The near-surface layer ionization takes place in polymers at the implantation and results in the formation of free radicals and other surface defects. Due to their high mobility in the radiation-damaged region of the polymer, light ions diffuse to the surface and are captured by these defects, the concentration of which is proportional to the electron damage of the target [25]. It was shown [26] that the transition from the regular distribution profile of the implanted impurity to the ionized one takes place when the contribution of the electron deceleration to total

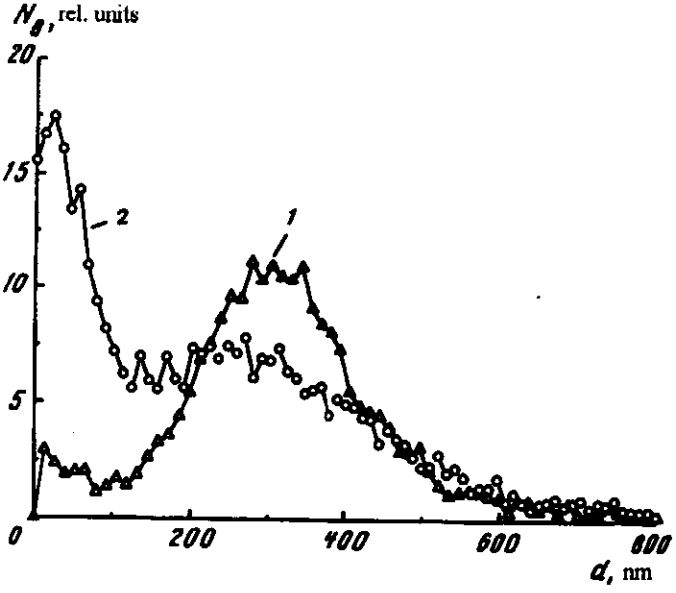

Figure 1. Distribution profiles in depth of boron implanted in polyethylene (*1*) and polyamide (*2*) with the energy of 100 keV and the dose of 5×10^{16} cm^{-2}.

energy losses becomes essentially higher than the nuclei deceleration ($S_e \approx (2-5)S_n$, where S_e and S_n are the values of energy losses per unit length for the electron and nuclei deceleration, respectively). It explains the dependence of distribution profiles of the introduced impurities on the implantation energy. At the same time, no essential influence of the implantation dose on the ion free-path was found up to the values of 10^{16} cm^{-2} [27].

The proper concentration gradient can be the diffusion basis. One can not exclude the possibility of electrodiffusion due to the potential difference between the implanted surface and the polymer inner layers. As far as the diffusion mechanism is concerned, one can suggest that impurities diffuse mainly along ion tracks trapping simultaneous atoms by the defects created.

The last hypothesis is confirmed by the experimental data on the impurity diffusion in implanted polymers and by the results on the distribution of boron implanted into polyethylene, polyamide and cellulose with the energy of 100 keV and doses $\geq 1\times10^{16}$ cm^{-2} (Fig. 1) obtained by NDP methods [28, 29]. The tracks overlap, when the doses are so high, and the diffusion processes proceed more intensively. This is evidenced by the experimental observation of the presence of the near-surface maximum of the boron concentration with the amplitude depending on the type of the polymer film in which the implantation was conducted. A dip in the boron concentration profile (Fig. 1) appears to be determined by structural changes in the implanted polymer layer [30] resulting in an essential decrease in the concentration of trapping centers of the impurity atoms migrating in this layer. The in-depth maximum of the boron concentration correlates well with the maximum of ion energy losses at the nuclei deceleration [29]. A similar effect was previously observed for various ion–target combinations. It reflects the ion redistribution

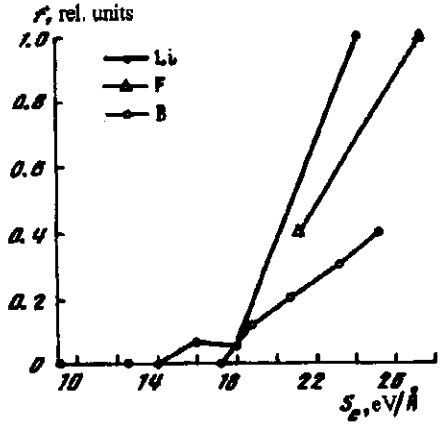

Fig. 2

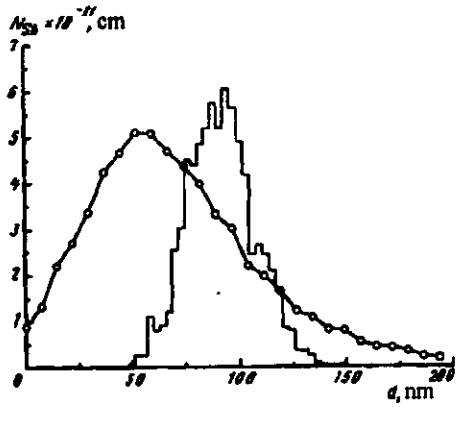

Fig. 3

Figure 2. Dependence of the value of the mobile fraction of light ions implanted in AZ111 photoresist on energy losses due to electron deceleration.

Figure 3. Depth distribution profiles of antimony implanted in polyethylene with the energy of 100 keV and the dose of 5×10^{16} cm^{-2}. The profile calculated by the TRIM program is presented as a histogram.

caused by diffusion immediately after implantation and their trapping by radiation-induced defects. From the other side, according to the calculations made for lithium ions implanted in polypropylene with the energy of 100 keV, one trapping of a migrating ion accounts for 1 keV of the energy loss [31]. This value is 2–6 times less than the radiation-stimulated chemical yield of destruction or joint of polymer chains. It follows that not each radiation defect is able to capture a diffusing atom. At the same time, according to the results given in the same work, the implanted impurity atom migration does not confine itself to ion tracks but can take place in the neighbor non-irradiated regions, although the diffusion rate is less there by at least an order of magnitude. It should be noted that in the case of the light ion implantation, their mobility becomes more essential (Fig. 2), when the ion deceleration by electrons is accompanied by an energy transfer to the polymer which exceeds a certain threshold value (for example, 16 ± 2 eV/Å at the implantation of B^+, Li^+ and F^+ ions in a photoresist). It provides a sufficient efficiency of radiation processes and the necessary level of the decrease in the target material density in the band of the implanted ion track [32].

As distinct from light ions, the distribution profiles in the depth of heavy ions implanted in polymers are close in shape to the regular, i.e. calculated ones. It is evidenced by the data of investigations of distribution profiles of a variety of ions ($9 \le Z \le 83$) implanted in photoresists AZ111 and AZ1350 in a wide range of energies and doses [27, 33]. However, the values of the average projected free-path of ions (R_p) are 20–25% less in experiments than in theoretical estimations, and the magnitudes of deviation from the average projected free-path (ΔR_p) exceed the calculated parameters by 75–100%. Herewith, R_p does not depend on the implantation dose, whereas ΔR_p grows with it. These results agree well with

the data presented in the works [20, 34, 5] on the implantation of As^+, Sb^+ and I^+ ions with energies of 50–150 keV and doses of 10^{13}–10^{15} cm^{-2} in polyethylene and polypropylene. It was found that the experimental R_p values are 25–30% less than the calculated data, and ΔR_p are 50–100% higher (Fig. 3). At the same time, no essential dependence of the profile parameters on the implantation dose was revealed. The authors ascribe the obtained deviations to the change in the polymer density at the implantation and to correlations between energy losses in the electron and nuclei deceleration which were neglected in the TRIM program.

It should be noted that there also exist literature data on the distribution of implanted ions in polymer materials which testify that the experimentally obtained ion free-path values can exceed the calculated values by 20–25% [33, 36]. This fact is an indication against the existing suggestion that the reason of deviation for the experimental values from theoretical ones is a charging of the polymer specimen at the implantation and an origin of the potential decelerating the impacting ions.

Recent investigations of the free-path of Au^+ and Bi^+ ions in carbon nitride (C:N = 75:25%) have demonstrated an excess of experimental R_p and ΔR_p values over the calculated results (TRIM-95) by 30% and by a factor of two, respectively [37]. The authors attempted to improve the interaction potential adapted for TRIM calculations by an introduction of a correction for energy losses ΔS_e due to the inelastic (electron) deceleration, its values being in the interval

$$-2\beta S_e \le \Delta S_e \le 0, \tag{1}$$

where $\beta = M_1/(M_1+M_2)$ and M_1 and M_2 are the masses of interacting particles. It is seen from (1) that this correction becomes essential when the value of β is close to unity or when the losses in the deceleration by electrons are comparable to those due to nuclei. Introduction of this correction in TRIM calculations allowed one to bring the rated ion free-path values much closer to the experimental ones. Thus, it has been proved that the introduction of heavy ions into a light matrix gives rise to a change in the relationship between energy losses in the electron and nuclei deceleration with respect to the known ZBL-model (Ziegler, Biersack, Littmark) used in the TRIM algorithm. It is one of the main reasons for the discrepancy between the parameters of the calculations and experiments.

Exceptions of the above-described results are the cases of the bombardment of polymers with inert gases, when the experimental R_p values differ more than two times from the calculated ones. For example, at the Ar^+ ions implantation the experimental magnitudes are 2–4 times less than calculated ones [38] The authors explained this effect by compacting the implanted layer. However, the more recent investigations of the same authors [39] have shown that at the low-temperature (90 K) implantation, the depth distribution profiles of ions of inert gases, in particular Xe, correspond to the calculated profiles with an accuracy of 10%. The temperature increase leads to the impurity diffusion which is slow in the radiation-damaged layer and enhanced in the intact region. This diffusion is responsible for the appearance of the so-called "tail" in the distribution profile in the depth of ions in polymers. According to the analysis performed, the behavior of xenon atoms obeys the following equation in the second case:

$$C(x, t) = C_0(\pi Dt)^{1/2}\exp(-x^2/4Dt), \quad (2)$$

where C_0 is the concentration of mobile Xe atoms, D the diffusion coefficient, x the diffusion depth. The values of the diffusion coefficient calculated on the basis of experiments correspond to the Arrhenius curves:

$$D = D_0\exp(-E_b/kT), \quad (3)$$

where the activation energy $E_b = 80$ meV.

Thus, the following view based on the diffusion mechanism in the implanted layer has been accepted to date. The impacting ions displace the atoms of the polymer macromolecule from their positions and form latent tracks (nanopores) or, in other words, certain "free volumes" or microcavities. The number of the microcavities will increase with the implantation dose so that they will overlap which will lead to an increase in the "free volume" stimulating enhanced impurity diffusion. Free radicals which are the effective trapping centers for the migrating impurity appear simultaneously [40], i.e. the diffusion is decelerated as if the preceding process was neutralized. The next implanted ions, again, promote the displacement of the trapped atoms due to the radiation-stimulated diffusion. Thus, the complex dynamic process of the radiation-stimulated diffusion based on the trapping-detrapping mechanism [41] occurs. In the implantation of light ions, the neutralization processes mainly characterize the single track regimes. When the tracks overlap becomes significant, the efficiency of trapping of the diffusing impurity by defects decreases, although the degree of the polymer damage grows with the dose and tends to saturation. The latter is well explained by carbonization processes. In the case of the implantation of inert gases, an essential role in the stimulation of diffusion process is played by the radiolysis effect [42], when additional microcavities arise due to the formation and escape of gas products from the polymer bulk through latent tracks. It was shown that the trapping probability is proportional to the implantation dose, whereas the displacement process depends essentially on the type of bombarding ions.

In the light of this model, the results presented in [43, 44] are of interest. Implantation of K^+ ions in polyacetylene, previously doped by $FeCl_3$ diffusion, was investigated in these works. The initial homogeneous distribution of the impurity changes radically after the implantation. A concentration maximum appears which coincides with the peak of the depth distribution of implanted ions. Herewith, a part of the impurity diffuses towards the surface and escape from the polymer. The authors explain these effects by the radiation-stimulated diffusion of atoms of the doping impurity and their capture by defects and free radicals generated by the implantation. It is necessary to note that the formed systems have a low stability, so that spontaneous "tailing" of the impurity profile determined by the diffusion of individual components takes place after some time (tens of days).

Overlapping of ion tracks, or, more precisely, of the corresponding defect clusters, does not yet occur at the implantation of heavy ions and ions with medium masses with doses less than 10^{13} cm^{-2} (this threshold is slightly higher for light ions). As a result, each next ion enters an intact polymer, and effects of the significant discrepancy between the experi-

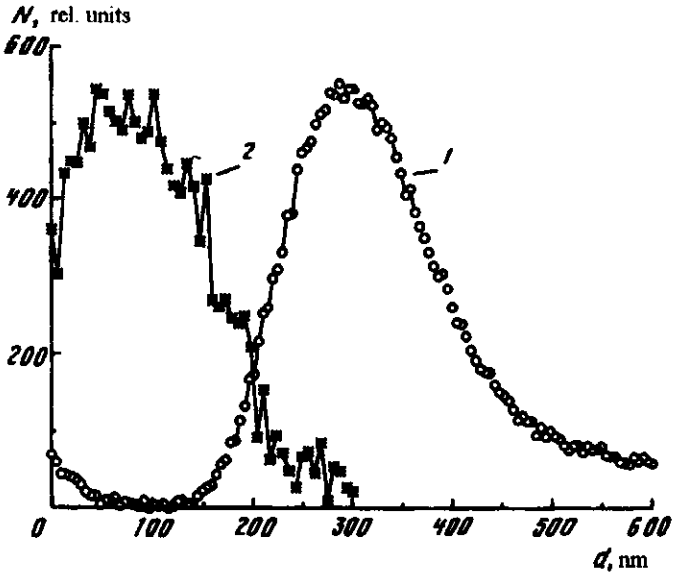

Figure 4. Depth distribution profiles of diffused iodine (*1*) and carbon "excess" (*2*) in polyethylene implanted with As^+ ions with the energy of 150 keV and the dose of 1×10^{15} cm^{-2}.

mental and theoretical results should be absent. However, the polymers implanted with small doses are inaccessible for the determination of the impurity depth profiles by the RBS method because of technical reasons (a low detected limit). The works [45–47] are interesting in this framework. In these works, in particular, the processes of defect formation in polyethylene implanted with F^+ and As^+ ions with the energy of 150 keV and in a wide dose range were investigated by decorating the ion tracks with iodine. It was established from RBS measurements that the iodine distribution in undoped samples is homogeneous down to the depth of 2 μm. The iodine profiles in depth have the concentration maximum in the implanted samples. The concentration value is an increasing function of the implantation dose up to values $\leq 1\times10^{14}$ cm^{-2}. Herewith, the depth distribution profiles J in polyethylene implanted with low doses (1×10^{12} cm^{-2}) are in a good agreement with the profiles of energy losses due to the electron deceleration calculated by the TRIM program, whereas the iodine depth profiles become closer to the profiles of energy losses due to the nuclei deceleration, when the implantation dose increases ($\geq 1\times10^{13}$ cm^{-2}). In the last case, an overlap of clusters of individual ions takes place, and the active process of dehydrogenization begins and is accompanied by the "free volumes" increase [48]. It results in the growth of the concentration of diffusing iodine which confirms the hypothesis of impurity penetration in the depth of the damaged polymer matrix along ion tracks. The iodine concentration decreases at the implantation doses of 5×10^{14} cm^{-2}–1×10^{15} cm^{-2} of F^+ and As^+ ions, its distribution has a pronounced inhomogeneous character and has two maxima, a surface (weakly marked) and internal one Fig. 4). The iodine distribution depth profiles do not correspond in this case to the profiles of energy losses due to either electron or nuclei decelerations of ions. It is caused by essential

structural changes in the polymer which occur at high implantation doses due to the development of the synthesis process of a carbonized phase and compacting of the polymer surface layer. These changes are accompanied by reduction of the number of trapping centers and, therefore, by the blocking of the diffusion. Therewith, the more the mass of implanted ions, the less is the implantation dose necessary to establish the barrier blocking the diffusion [49]. As is seen from Fig. 4, the iodine-depleted layer corresponds well to the strongly carbonized (due to the implantation) near-surface region of the polymer film.

Investigation of the adsorption of Pb^{2+} ions introduced by the diffusion in the implanted polyethylene also showed that a drastic fall in the diffusion coefficient of ions in pores and a decrease in the adsorption capacity of the ion-implanted layer [50] similar to that observed in the case of the iodine adsorption, occur when the implantation doses are larger than the carbonization threshold. Thus the pronounced adsorption properties are characteristic, first of all, for the samples implanted in the regime of "single tracks". As for the diffusion of complex compounds [51, 52] in the ion-implanted polymers, these results are somewhat different. For example, a separate diffusion of cations and anions of the initial compound was observed in the case of the introduction of $[(C_2B_9H_{11})_2Co]Cs$ metal carbonate in the implanted polyethylene [51] and led to both a change in the B/Cs ratio in the impurity stoichiometry and a difference in concentration depth profiles of individual elements. However, the nature of adsorption centers in the implanted layer remains unclear, the more so that the sorption of molecular iodine and ions from the solution seem to be provided by different centers.

The increase in the energy of implanted ions to hundreds of megaelectron-volts leads to a significant increase in the size of pores (ion tracks) and, in particular, makes it possible to dope the implanted layer with fullerenes. In the case of polyimide implanted with J^{22+} ions with the energy of 500 MeV, the concentration of C_{60} molecules diffusing spontaneously in the implanted layer from the toluene solution reaches 1.8×10^7 molecules of C_{60} per one track [22] (the concentration of C_{60} was determined by the NDP method, where lithium ions forming an insoluble compound with C_{60} were used as a marker).

Alongside with the diffusion, the phenomenon of backward sputtering of ions from the surface of a polymer specimen appearing in the case of extremely high implantation doses ($\geq1\times10^{17}$ cm^{-2}) of heavy ions, e.g. As^+ and Xe^+ [53], can play an important role in deviation of the experimentally obtained values of the implanted impurities concentration from the calculated values. It is established that in the implantation of arsenic with the dose of 2×10^{17} cm^{-2} its concentration in the layer is 7.6×10^{16} cm^{-2}, i.e. only 39 at. %. In the implantation of Xe ions with the doses of $(1-2)\times10^{17}$ cm^{-2}, its layer concentration was 5.5×10^{15} cm^{-2}. Such a low value cannot be explained by sputtering only, since, according to the TRIM program, the sputtering factor is 0.43 atom/ion for 50 keV Xe^+ ions in the polymer. This value only slightly exceeds the value of 0.3 atom/ion characteristic for the implantation of As^+ ions. It seems likely that most of the implanted xenon ions form a gas phase, the most part of which diffuses quickly to the surface and escapes from the polymer bulk. At the same time, as follows from RBS spectra, 10–20% of xenon is revealed beyond the implanted layer. It bears witness to the diffusion in the depth of the intact polymer and agrees with the data presented above.

The comprehensive analysis of the results presented above allows us to conclude that deviations of the experimental magnitudes of the ion path length from the calculated values

are due to a series of factors. First of all, these are essential changes in the structure, composition and density of the polymer surface layer during implantation which are not taken into account in the model representations because of both the absence of the certain data on such transformations, i.e. *in situ* measurements, and the complexity of modeling such changes. Furthermore, correlations between the energy losses due to the electron and nuclei deceleration are neglected in the algorithms used in calculations. The diffusion processes proceeding immediately after implantation or directly with it, and the backward ion sputtering at the extremely high doses play a certain role in some cases.

A CHANGE IN THE POLYMER STRUCTURE AND COMPOSITION AT ION IMPLANTATION

The action of the ion implantation on the structure and composition of polymers is a sophisticated complex of physical and chemical processes and phenomena including the interaction between the impacting ions and the polyatomic target, as well as radiation and pyrolytic transformation processes of the polymer matrix. The characteristics of these phenomena depend on the energy transferred to the polymer at the implantation, on the composition and structure of the polymer itself, its interaction with the environment before and after the ion implantation etc.

The presence of two principally different mechanisms of the energy transfer from implanted ions to the polymer which proceeds by electron excitation and nuclear collisions, dominantly influences the course of the ion-induced chemical processes taking place in polymer materials. Allowance for the electron or nuclear interaction by which the energy transfer from implanted ions to the polymer matrix is realized, has the principal meaning for understanding the mechanism of chemical modifications of polymers at the ion implantation. Indeed, whereas nuclear collisions are accompanied by the direct breaking of chemical bonds, electron interactions result in the excitation of the macromolecule fragments. If one takes into account that the noticed excited state can migrate through a long distance for its life time ($\sim 10^{12}$ c), one can expect that the weakest bonds will be broken first in the case of the energy transfer by the electron deceleration. The role of such effects is especially significant in the case of the ion implantation of heteropolychain compounds. Evidently, the break of chemical bonds will have principally a statistical character in the case of the nuclear mechanism of the energy transfer, whereas the destruction of extended electron systems having a high delocalization level in the conditions of the electron deceleration, as well as under the action of mobile active particles (first of all, $H^{\cdot}$ radicals) will be distinctly selective. For example, at the ion implantation of polyimide with light ions (under conditions when the ratio S_n/S_e does not exceed 0.15), the ethereal bond between aromatic cycles degrades first [54], and the imide groups transform progressively into the amide ones without breaking the polymer chain [55]. The increase in the specific weight of nuclear losses in the process of the energy transfer from the impacting ions fundamentally influences the character of the processes taking place in the polymer target. For example, at the implantation of polysulfone with As^+ ions with the energy of 50 keV (S_n/S_e = 5–6 in this case), not only the sulfone group is broken, but acetylene splits out and gives rise to the formation of 1.4-substituted butadiene [56].

Thus, the consequence of the polymer implantation is its degradation due to modification of chemical bonds, namely, destruction of molecular polymer chains (fraction formation) and their branching and the formation of free radicals which, closing on themselves, form transverse intermolecular and conjugate bonds [57]. The intensity of the destruction or branching processes is closely connected to the polymer type. For example, molecular chain fraction formation is the most characteristic of polyisobutylene, whereas polyethylene and polystyrene are characterized by branching and the formation of transverse bonds. When the number of transverse bonds attains a certain critical value, insoluble gel fractions with a three-dimensional network of transverse bonds between macromolecules begin to form [58]. The groups with the strong bond (for example, CCl, CO, CN or others depending on the type of the organic substance) can trap an electron at the fragmentation and form a negatively charged ion. The ions and free radicals generated at the implantation can further participate in chemical reactions proceeding by diffusion. Free radicals usually originate in pairs when molecules are split. Ions and free radicals can recombine with electrons or with each other, and the recombination rate depends on their concentration and mobility. The mobility of ions and free radicals in polymers is small.

The kinetic energy transferred to the target atoms at the interaction with the impacting ions and displaced atoms (playing the role of secondary bombarding particles) can lead to a process of an abrupt temperature increase [59]. Estimates made in the framework of the model of "thermal wedge" [60], show that the T value is of the order of 104 K for ions implanted in polymers with the energies from 100 keV to 1 MeV. Herewith, the temperature falls to the level of the target temperature settled at the implantation (350 K) for 10^{-9}–10^{-10} s. The estimates obtained in this way are very rough but permit one to envisage the character of thermal effects at the ion bombardment of polymers. It should be specially noted that the chemical processes taking place in the polymer matrix at the ion implantation can not be reduced either to thermal (in spite of the high peak temperature in the track) or to pure radiation effects and are a common process of radio-thermolysis.

Since the thermal conductivity coefficients of polymers is small, the radiolysis phenomenon (an analogue of pyrolysis) will occur in the conditions of high temperatures and the generation of many broken bonds. It will be followed by escape of the highly volatile gas products from the radiation damaged layer [57, 59], e.g. C_2H_2, CH_4, H_2 from polyethylene, polypropylene and polystyrene, C_2H_2, H_2, O, CO_2 from polyimides, C_2F_4, C_2F_4 from Teflon and so on. Therewith, the escape of H_2 results in dehydrogenization and formation of free radicals, of CO – in amidation, of CO_2 – in dissociation of carboxyl groups and so on.

The degassing processes are not linear because of their dependence on the ion implantation dose, ion penetration depth and relationship between energy losses due to the nuclei and electron deceleration.

The consequence of degassing processes is enrichment of the implanted layer with carbon, i.e. carbonization. Since the target surface enrichment with carbon is observed in RBS spectra as the change on the background of the signal corresponding to the carbon content in the initial sample, it is possible to follow the kinetics of carbonization beginning from doses of 1×10^{14} cm^{-2}. The profile of the carbon concentration change in the surface layer of the polymer at the implantation which is reconstructed from the "differential" RBS-spectrum, as a rule, has a maximum which is especially well marked in the case of

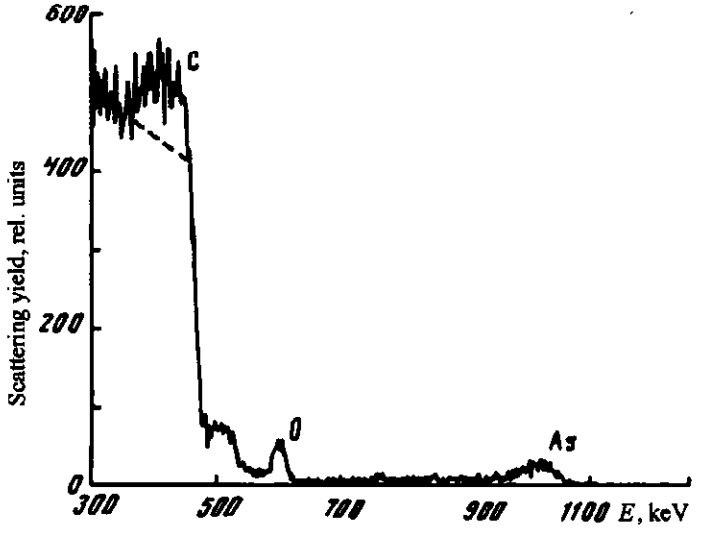

Figure 5. RBS spectrum of polyethylene implanted with As^+ ions with the energy of 150 keV and the dose of 1×10^{15} cm^{-2}.

implantation of heavy atoms [20, 21, 35] (Fig. 5) and located at a certain depth under the surface. This effect can be explained by the dominance of nuclei deceleration processes and, as a result, by more significant heat release at the end of the track of implanted ions, and by the lateral widening of the thermolysis zone in the regions of cascades of knocked out atoms which causes a displacement of the carbonization region deep in the polymer target.

It is essential that the ion bombardment does not result in the complete carbonization of the polymer surface. So, at the implantation of polyethylene with F^+ ions with the energy of 150 keV, the carbon concentration in the implanted layer comes to saturation at the level of 40 at. % [56] (as compared to 33% in the initial polyethylene). The degree of polymer dehydrogenization caused by the implantation increases rapidly in this energy interval, as the nuclear mechanism of the energy transfer becomes more important in total energy losses of impacting ions. For example, the carbon content reaches 65 at. % in the case of polyethylene implanted with As^+ ions with the energy of 150 keV, and 75 at. % in the case of the implantation of iodine ions in propylene [20, 21]. An increase in the carbon content from 52 to 83% at the implantation of As^+ ions with the dose of 1×10^{16} cm^{-2} in polyamidimide was found also in the work [61]. According to other data [50], the hydrogen content can fall to 15 at. % after the additional lead diffusion in polyethylene samples implanted with high doses of heavy ions. The process of the ion-induced carbonization of polymers at the implantation of heavy ions is practically accomplished, as a rule, at the dose level from 5×10^{15} to 1×10^{16} cm^{-2}. The surface structure and composition of the implanted polymer change only slightly at a further increase of the dose. Only the cases of surface sputtering under bombardment with heavy ions in the regime of doses higher than 1×10^{17} cm^{-2} are an exception.

Carbonization of the radiation-damaged layer is observed at the implantation of light ions in polymers at higher doses than in the case of heavy ions. According to the results of the work [30], where the boron implantation in polyethylene and polyamide was investigated, these doses are higher than 1×10^{16} cm^{-2}. A low efficiency of dehydrogenization in the range of high doses when the electron deceleration is dominant (namely, it dominates at the implantation of light ions) can be explained by the effective delocalization of excitation in graphite-like networks of carbon clusters and an increase of the cooling rate in the thermal wedges due to the higher value of thermal conductivity of the carbonized polymer. For the same reason, a noticeable concentration of heteroatoms is kept in the implanted layer even at high doses. As a result of the implantation, they turn out to be connected in more stable groups than in the initial polymer. The direct bond destruction under the conditions of nuclear collisions appears to be more effective from the viewpoints of both deep dehydrogenization of polymers and the destruction of free-carbon groups. The carbonization degree reached under such conditions is determined by the effects of retrapping of atomic hydrogen on broken carbon bonds.

The high level of dehydrogenization of the implanted polymer (the content of bound hydrogen being less than 10%) can also be achieved in the case of the pure electron mechanism of the ion deceleration. However, the use of ions with the energy of tens of mega-electron-volts is necessary for this purpose [62]. Since the sites of the growth of the carbon phase are in this case on the edges of the growing clusters (under conditions of excitation delocalization, the process of dehydrogenization and broken bond formation is located precisely here), the material with the vibration spectrum similar to that of implanted graphite is formed at the high-dose implantation [63].

In the work [62] it was shown by using the original technique of the small-angle neutron scattering that two types of structures based on unbound carbon emerge in the polyethylene terephthalate layers subjected to the high-energy implantation with boron ions (50 MeV): carbon formations with the average sizes of 6–7 nm and the distance of 13 nm between them; spherical coagulates, 10–50 nm in diameter and with the distance of 0.1–20 nm between the surfaces. The formation of carbon inclusions with the sizes of the order of 40 nm was also observed after irradiation of polymer films with boron, nitrogen and carbon ions with the dose of 3×10^{15} cm^{-2} and energy of 400–700 keV [64]. These results agree well with the model of the formation of pyrocarbon "drops" proposed in [28, 30] based on the investigations of the ion implantation in a series of polymer materials. According to this model the overall geometry of the damaged region is a tree-like structure (a cluster) analogous to that obtained at the implantation of inorganic semiconductors. The region of the elevated temperature is formed around the ion track at the implantation (when a part of the kinetic energy transforms into the thermal one). Due to the low thermal resistance of polymers, the cluster thermolysis takes place and results in the formation of pyrolysis drop-shaped inclusions enriched with carbon and surrounded with a π-electron "coat". Spectroscopic measurements and calculations made on their basis [28] show that the "drop" sizes increase with the implantation dose and achieve 2 nm when the boron or nitrogen implantation dose is of the order of 10^{17} cm^{-2}. These "drops" can react with each other forming covalent C=C-bonds. At high implantation doses, an overlap of drops and formation of a continuous pyrolysis layer enriched with carbon and characterized by the presence of conjugate C=C-bonds, will occur. The difference in the sizes of carbon

inclusions, as compared to those indicated in the works [62, 64], is due to lower implantation energies. The depth of an occurrence of carbonized layers and their thickness depend on the implantation energy and the ion type. It was shown [5, 30, 65] that these layers are responsible for the increase of the conductivity of implanted polymers. Therefore it is possible to create layer structures of the "polymer/conducting layer/polymer" type and operating electronics elements on this basis, e.g. resistors, diodes [66], switching elements [5, 65, 67], temperature sensors [68] and so on.

The above-considered examples allow us to conclude that the process of polymer modification at the ion implantation includes the following basic stages corresponding to certain dose ratings:

(1) creation of initial structural elements for the formation of the carbonized phase (carbon clusters of a small size, non-limiting compounds, macroradicals) which proceeds on the background of the radiation lacing of the polymer and release of volatile components;

(2) growth of carbon clusters;

(3) link formation between clusters, their aggregation until the formation of a continuous pyrolysis carbon-rich layer.

A certain change of the implanted layer composition and its structural-morphological features corresponds to each of these stages. One should note that carbon structures generated at the implantation reinforce the polymer surface which results in a significant increase of hardness [12, 13].

For all polymer samples the matrix of which does not contain oxygen, after the implantation the oxidation of the surface radiation-damaged layer was observed which takes place during the ion implantation (residual O_2 in the implanter chamber) or after it (oxygen contained in air). The oxygen content and profiles of its depth distribution depend on the dose, the implantation energy, the type of the implanted ions and polymer type, too. It should be noted that the dynamics of the oxygen concentration variation in the implanted layer does not change qualitatively as a function of the energy and type of implanted ions in the case of polymer films implanted with heavy ions [20, 35]. The oxygen content grows with the implantation dose and reaches a maximum at the doses of $(1-5)\times10^{14}$ cm^{-2}. Herewith, the O-atoms distribution is not homogeneous and has a maximum (Fig. 6). The dominant role in the oxidation process is played by trapping oxygen penetrating in the radiation-damaged layer on molecular fragments, free radicals and defects of other kinds [57]. Therefore, the maximum oxygen concentration is observed in the region of maximum energy losses of implanted ions in the case of both the nuclei and electron deceleration. A capability of each of these mechanisms to provide the generation of broken carbon bonds depends on the implantation dose, since at low dose ratings, when the undamaged or weakly damaged polymer is subjected to implantation, the formation of stable and metastable radicals is due to the electron deceleration. At the high-dose implantation (that is when the polymer is already carbonized), the broken carbon bonds are formed mainly in the nuclear collisions, whereas the energy transferred to the target by the electron deceleration mechanism dissipates efficiently in carbon structures. Therefore even in the case of heavy ions for which $S_n >> S_e$, the depth distribution profile of captured oxygen decorating radical centers corresponds at low implantation doses ($\leq 10^{13}$ cm^{-2}) to the profile of energy losses at the electron deceleration, and at higher doses – to that at nuclei

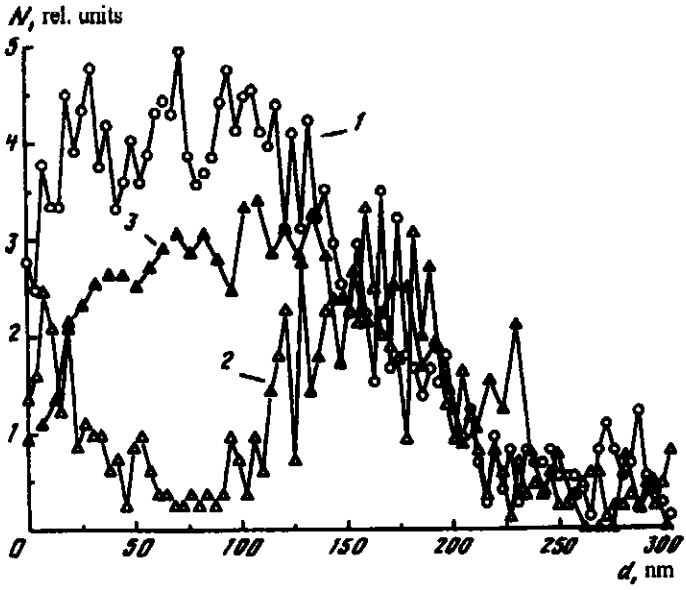

Figure 6. Depth distribution profiles of oxygen in polyethylene implanted with As^+ ions with the energy of 150 keV and doses of 1×10^{14} cm^{-2} (*1*) and 1×10^{15} cm^{-2} (*2*), and the profile of carbon "excess" after implantation with the dose of 1×10^{15} cm^{-2} (3).

deceleration [45]. The oxygen penetrating to the layer damaged by implantation reacts with free radicals and creates relatively stable products. It was shown many times by the infrared spectroscopy technique that a significant part of incorporated oxygen forms carbonyl groups. The last investigations have shown that ion tracks produced by implantation are precisely the channels by which oxygen enter polymer samples. Therewith, the diffusion of the oxygen atoms is not confined to the near-surface implanted region but also proceeds in the depth of the non-modified material.

When implantation doses of heavy ions are more than 5×10^{14} cm^{-2}, the depth distribution profile of O atoms which has two maxima changes abruptly (Fig. 6), and the total oxygen concentration in the modified layer decreases noticeably. The surface maximum is probably connected with trapping of oxygen on defects, formed at the electron deceleration, as well as with skin-effects, whereas the deep maximum may be due to the defect formation at the process of nuclei deceleration. The oxygen depletion of the central part of the profile can be associated with significant changes in the layer structure and composition, in particular, the above-described carbonization effect, because the maximum of the carbon "excess" concentration corresponds to the minimum of the oxygen content (Fig. 6). However, the detailed relationship between these processes requires further investigation.

The qualitatively different relation between oxidation processes and the dose increase was found in the case of the light ion implantation, for example, fluorine [35, 69] and boron [30]. A monotonous increase in the oxygen concentration with the dose is observed up to the value of 1×10^{16} cm^{-2} in these cases. Herewith, the oxygen distribution in the depth of

the implanted layer is approximately homogeneous. A further increase of the dose is accompanied by an essential oxygen depletion of the near-surface layer. Note that in contrast to the case of the heavy ion implantation, the surface peak of the oxygen concentration is absent. As was noted above, it is likely to be due to the diffusion of the implanted light ions and their incorporation near the surface which prevents an accumulation of oxygen in this region. Other data [70] indicate that oxygen can expel impurities, which were previously introduced in the polymer and chemically bound, from the near-surface implanted region. It happened, for example, in the case of the He^+ ion implantation in polyethylene containing Li, when the oxygen content in the polymer increased to 20% in the result of implantation, and the front of the lithium depth distribution shifted towards the specimen surface. In some cases the effects of liberation of gas products from the track volume and changes of the polymer density at the local thermolysis cannot provide a high permeability of the implanted layer, and the slow diffusion of oxygen takes place along radiation defects emerging in the track of implanted ions. For example, the velocity of the oxidation front in the implanted layer does not exceed 4×10^{-5} nm/s in ion-modified polypropylene [21], so that tens of days are necessary to accomplish oxidation if the polymer is kept in air [34].

It can be concluded from the above-said that at high implantation doses called the threshold doses (more than 5×10^{14} cm^{-2} for heavy ions, and 1×10^{16} cm^{-2} for light ions) the structure and composition of the radiation-damaged layer of polymers change essentially. It is characterized by overlap of low-dimensional structures (clusters, "drops") enriched with carbon (to the point of the formation of a continuous pyrolysis layer). It promotes a significant decrease in the number of trapping centers of both oxygen and migrating atoms of the implanted impurity. The formation of individual low-dimensional carbon-containing clusters is characteristic for the below-threshold doses, but the processes of oxidation of the implanted surface layer of the polymer with the formation of carbonyl groups play the dominant role.

CONCLUSIONS

The overview given in the present work and the critical analysis of the data on implantation of polymer materials are testimony to the following:

(1) the ion free-path and their final depth distribution are influenced, first of all, by an essential variation of the structure and composition of polymers at the implantation, especially at high doses, and also by diffusion processes, including the radiation-stimulated diffusion which proceeds both in the process of implantation and for a short time after it;

(2) the structural changes of polymers manifest themselves in fragmentation and splitting of polymer chains, the emergence of low-molecular fragments, free radicals, degassing, formation of conjugate double bonds and new compounds, carbonization and oxidation;

(3) in the range of low dose ratings ($< 10^{14}$ cm^{-2}) corresponding to the one-fold filling of the specimen surface with ion tracks, the primary products formed in the polymer are the lowest non-limiting compounds (playing the role of radiation defects) and carbon clusters; the broken carbon bonds not used at the formation of these products are compensated effectively by the interaction with oxygen which diffuses along latent tracks with the formation of carbonyl groups;

(4) at the implantation doses which can be called threshold ($>5\times10^{14}$ cm^{-2} for heavy ions and $>1\times10^{16}$ cm^{-2} for the light ones) and over-threshold, the process of the formation of carbon structure in the course of interaction and overlap of the growing carbon clusters in polymers becomes prevailing. It leads to a significant decrease in the number of centers of oxygen trapping in the implanted layer and the termination of the process of the formation of the continuous near-surface carbonized layer with a branching network of conjugate carbon bonds providing delocalization of a large number of π-electrons and, therefore, high values of conductivity in this layer;

(5) it is possible to form hidden conducting layers lying at a depth which can be controlled by choosing the type of ions and implantation energy and to obtain layer structures of the "polymer/conducting layer/polymer" type in order to create operating elements of microelectronics on this basis;

(6) there exists a wide base of the experimental data on the structural reconstruction of polymers which is a basis for the development of the view on mechanisms of transport of charge carriers and the theory of conductivity of implanted polymers;

The enumerated conclusions point out a series of promising directions both in the development of fundamental problems of radiation physics and chemistry of polymers and diverse practical applications of implantation-modified polymer materials.

REFERENCES

1. F. H. Winslow, W. O. Baker, and W. A. Yager, *J. Amer. Chem. Soc.*, **77**: 475 (1955).
2. S. D. Levina, K. P. Lobanova, A. A. Berlin, and A. I. Sherle, *Dokl. Akad. Nauk SSSR, Ser. Khim.*, **145**: 602 (1962) (in Russian).
3. *Electrical Properties of Polymers*, ed. B. I. Sazhin (Leningrad: Khimia) (1986) (in Russian).
4. I. H. Loh, R. W. Oliver, and P. Sioshansi, *Nucl. Instrum. Meth.*, **B34**: 337 (1988).
5. V. B. Odzhaev, V. N. Popok, I. A. Karpovich, *et. al.*, *Izv. Belorusskoi inzhenernoi akad.* : no. 1(3)/3, 214 (1997) (in Russian).
6. A. Moliton, B. Lucas, C. Moreau, *et al.*, *Phil. Mag.*, **B69**: 1155 (1994).
7. H. Stabb, E. Punkka, and J. Paloheimo, *Mater. Sci. Engng.*, **10**: 85 (1993).
8. V. Švorčik, R. Endrst, V. Rybka, *et al.*, *J. Electrochem. Soc.*, **140**: 542 (1993).
9. D. Fink, M. Muller, L. T. Chadderton, *et al.*, *Nucl. Instrum. and Meth.*, **B32**: 125 (1988).
10. L. Zhang, P. D. Townsend, P. J. Chandler, and J. R. Kulisch, *J. Appl. Phys.*, **66**: 4547 (1989).
11. S. Brunner, D. M. Ruck, W. F. X. Frank, *et al.*, *Nucl. Instrum. and Meth.*, **B89**: 373 (1994).
12. E. H. Lee, G. R. Rao, M. B. Lewis, and L. K. Manzur, *Nucl. Instrum. and Meth.*, **B74**: 326 (1993).
13. R. Ochsner, A. Kluge, Zechel-Malonn, *et al.*, *Nucl. Instrum. and Meth.*, **B80/81**: 1050 (1993).
14. J. D. Carlson, J. E. Bares, A. M. Guzman, and P. P. Pronko, *Nucl. Instrum. and Meth.*, **B7/8**: 507 (1985).
15. Y. Suzuki, M. Kusakabe, H. Akiba, *et al.*, *Nucl. Instrum. and Meth.*, **B59**: 698 (1991).
16. V. Havranek, V. Hnatowicz, J. Kvitek, and V. Perina, *Nucl. Instrum. and Meth.*, **B72**: 224 (1992).
17. V. Hnatowicz, V. Havranek, and J. Kvitek, *Nucl. Instrum. and Meth.*, **B53**: 337 (1991).
18. J. Kvitek, V. Hnatowicz, and P. Kotas, *Radiochem. Radioanal. Lett.*, **24(3)**: 205 (1976).
19. J. Davenas, X. L. Xu, G. Boiteux, and D. Sage, *Nucl. Instrum. and Meth.*, **B39**: 754 (1989).
20. V. Hnatowicz, J. Kvitek, V. Švorčik, and V. Rybka, *Eur. Polym. J.*, **29**: 1255 (1993).
21. V. Hnatowicz, J. Kvitek, V. Švorčik, and V. Rybka, *Appl. Phys.*, **A58**: 349 (1994).
22. D. Fink, R. Klett, C. Mathis, *et al.*, *Nucl. Instrum. and Meth.*, **B100**: 69 (1995).
23. J. F. Ziegler, J. P. Biersack, and U. Littmark, *The Stopping and Range of Ions in Solids.* (New York, Pergamon Press) (1985).

24. D. Fink, J. P. Biersack, and J. T. Chen, *J. Appl. Phys.*, **58**: 668 (1985).
25. R. B. Guimaraes, L. Amaral, M. Behar, *et al.*, *J. Appl. Phys.*, **63**: 2083 (1988).
26. R. B. Guimaraes, M. Behar, R. P. Livi, *et al.*, *J.Appl. Phys.*, **60**: 1322 (1986).
27. R. B. Guimaraes, M. Behar, R. P. Livi, *et al.*, *Nucl. Instrum. and Meth.*, **B19/20**: 882 (1987).
28. V. N. Popok, V. B. Odzhev, I. P. Kozlov, *et al.*, *Nucl. Instrum. and Meth.*, **B129**: 60 (1997).
29. J. Vacik, J. Cervena, D. Fink, *et al.*, *Radiation Effects and Defects in Solids*, **143**: 139 (1997).
30. V. B. Odzhaev, I. I. Azarko, I. A. Karpovich, *et al.*, *Mater. Lett.*, **23**: 163 (1995).
31. D. Fink, M. Behar, J. Kaschny, *et al.*, *Appl. Phys.*, **A62**: 359 (1996).
32. D. Fink, L. T. Chadderton, S. A. Cruz, *et al.*, *Radiation Effects and Defects in Solids*, **132**: 81 (1994).
33. M. Behar, P. L. Grande, L. Amaral, *et al.*, *Phys Rev.*, **B41**: 6145 (1990).
34. V. Hnatowicz, V. Havranek, J. Kvitek, *et al.*, *Jpn J. Appl. Phys.*, **32**: 1810 (1993).
35. V. Hnatowicz, J. Kvitek, V. Švorčik, *et al.*, *Czech. J. Phys.*, **44**: 621 (1994).
36. R. G. Wilson, *J.Appl. Phys.*, **73**: 2215 (1993).
37. J. R. Kaschny, M. E. Perez, M. Behar, *et al.*, *Nucl. Instrum. and Meth.*, **B122**: 8 (1997).
38. R. B. Guimaraes, M. Behar, R. P. Livi, *et al.*, *Nucl. Instrum. and Meth.*, **B19/20**: 882 (1987).
39. M. Behar, L. Amaral, J. R. Kaschny, and F. C. Zawislak, *Phys.Lett.*, **A148**: 104 (1990).
40. M. Behar, L. Amaral, J. R. Kaschny, *et al.*, *Nucl. Instrum. and Meth.*, **B46**: 313 (1990).
41. J. R. Kaschny, L. Amaral, D. Fink, and M. Behar, *Rad. Effects and Defects in Solids*, **125**: 289 (1993).
42. H. B. Luck, *Nucl. Instrum. and Meth.*, **202**: 497 (1982).
43. W. M. Wang, H. H. Wan, T. W. Rong, *et al.*, *Nucl. Instrum. and Meth.*, **B61**: 466 (1991).
44. S. H. Lin, K. L. Sheng, T. W.Rong, *et al.*, *Nucl. Instrum. and Meth.*, **B59/60**: 1257 (1990).
45. O. Jankovskij, V. Švorčik, V. Rybka, *et al.*, *Nucl. Instrum. and Meth.*, **B95**: 192 (1995).
46. V. Hnatowicz, J. Vacik, V. Perina, *et al.*, *Rad. Measurem.*, **25(1–4)**: 71 (1995).
47. V. Hnatowicz, J. Vacik, V. Švorčik, *et al.*, *Nucl. Instrum. and Meth.*, **B114**: 81 (1996).
48. V. Švorčik, V. Rubka, O. Jankovskij, and V. Hnatowicz, *J. Appl. Pol. Sci.*, **61**: 1097 (1996).
49. J. Davenas and X. L. Xu, *Nucl. Instrum. and Meth.*, **B71**: 33 (1992).
50. V. Hnatowicz, J. Kvitek, V. Perina, *et al.*, *Nucl. Instrum. and Meth.*, **B93**: 282 (1994).
51. V. Hnatowicz, J. Vacik, J. Cervena, *et al.*, *Nucl. Instrum. and Meth.*, **B105**: 241 (1995).
52. L. Calcagno, R. Percolla, and G. Foti, *Nucl. Instrum. and Meth.*, **B91**: 426 (1994).
53. Y. Wang, S.S. Mohite, L.B. Bridwell, *et al.*, *J.Mater. Res.*, **8(2)**: 388 (1993).
54. J. Davenas, X. L. Xu, G. Boiteux, and D. Sage, *Nucl. Instrum. and Meth.*, **B39**: 754 (1989).
55. V. Švorčik, R. Endři, V. Rubka, *et al.*, *Eur. Polym. J.*, **31**: 189 (1995)
56. L. B. Bridwell, R. E. Griedd, W. Yongqiang, *et al.*, *Nucl. Instrum. and Meth.*, **B59/60**: 1240 (1991).
57. A. Chapiro, *Nucl. Instrum. and Meth.*, **B32**: 111 (1988).
58. L. Calcagno, R. Percolla, and G. Foti, *Nucl. Instrum. and Meth.*, **B95**: 59 (1995).
59. M. B. Lewis and E. H. Lee, *Nucl. Instrum. and Meth.*, **B61**: 457 (1991).
60. I. S. Bitensky, P. Demirev, and B. U. R. Sundquist, *Nucl. Instrum. and Meth.*, **B82**: 356 (1993).
61. Y. Wang, S. S. Mohite, L. B. Bridwell, *et al.*, *J. Mater. Res.*, **8(2)**: 388 (1993).
62. D. Fink, K. Ibel, P. Goppelt, *et al.*, *Nucl. Instrum. and Meth.*, **B46**: 342 (1990).
63. C. J. Sofield, S. Sugden, J. Ing, *et al.*, *Vacuum*, **44**: 285 (1993).
64. R. G. Rao, Z. L. Wang, and E. H. Lee, *J. Mater. Res.*, **10**: 927 (1993).
65. I. I. Azarko, I. A. Karpovich, I. P. Kozlov, *et al.*, *Proc. of Scientific Conf. at 75-year Anniversary of BGU* (Belorussian State University), (Minsk, BGU), **1**: 158 (1996) (in Russian).
66. W. M. Wang, H. H. Wan, T. W. Rong, *et al.*, *Nucl. Instrum. and Meth.*, **B61**: 466 (1991).
67. I. I. Azarko, I. A. Karpovich, I. P. Kozlov, *et al.*, *Proc.of Internat. Symp. "Ion Implantation of Science and Technology"*. Jan. 22–24, 1997 (Naleczow, Lublin Technical University) (1997).
68. R. F. Giedd, M. G. Moss, M. M. Craig, and D. E. Robertson, *Nucl. Instrum. and Meth.*, **B59/60**: 1253 (1991).
69. V. Hnatowicz, V. Havranek, J. Kvitek, *et al.*, *Nucl. Instrum. and Meth.*, **B80/81**: 1059 (1993).
70. D. Fink, R. Klett, M. Müller, *et al.*, *Appl. Phys.*, **A63**: 441 (1996).